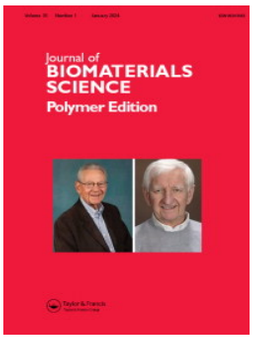

Journal of Biomaterials Science, Polymer Edition

ISSN: (Print) (Online) Journal homepage: www.tandfonline.com/journals/tbsp20

Characterization of gelatin-based wound dressing biomaterials containing increasing coconut oil concentrations

Mehlika Karamanlioglu & Serap Yesilkir-Baydar

To cite this article: Mehlika Karamanlioglu & Serap Yesilkir-Baydar (2024) Characterization of gelatin-based wound dressing biomaterials containing increasing coconut oil concentrations, Journal of Biomaterials Science, Polymer Edition, 35:1, 16-44, DOI: 10.1080/09205063.2023.2265624

To link to this article: https://doi.org/10.1080/09205063.2023.2265624

Published online: 11 Oct 2023.

JOURNAL OF BIOMATERIALS SCIENCE, POLYMER EDITION
2024, VOL. 35, NO. 1, 16–44
https://doi.org/10.1080/09205063.2023.2265624

Characterization of gelatin-based wound dressing biomaterials containing increasing coconut oil concentrations

Mehlika Karamanlioglu[a] and Serap Yesilkir-Baydar[a,b]

[a]Department of Biomedical Engineering, Istanbul Gelisim University, Istanbul, Turkey; [b]Life Sciences and Biomedical Engineering Application and Research Center, Istanbul Gelisim University, Istanbul, Turkey

ABSTRACT

This study determined the influence and ideal ratios of various coconut oil (CO) amounts in gelatin (G) based-films as wound dressings since there are limited comparative studies to evaluate the sole effect of increasing CO on protein-based biomaterials. Homogenous films at G:CO ratio of 4:0,4:2,4:3,4:4 (w:w) corresponding to CO-0, CO-2, CO-3, CO-4, respectively, were obtained using solution casting. SEM showed CO caused rougher surfaces decreasing mechanical strength. However, no pores were observed in CO-4 due to bigger clusters of oil improving stretchability compared to CO-3; and durability since aging of CO-4 was >10% lower than CO-0 in aqueous media. FTIR showed triglycerides' band only in CO films with increasing amplitude. Moreover, amide-I of CO-2 was involved in more hydrogen bonding, therefore, CO-2 had the highest melt-like transition temperatures (Tmax) at ~163 °C while others' were at ~133 °C; and had more ideal mechanical properties among CO films. XTT showed that increased CO improved 3T3 cell viability as CO-0 significantly decreased viability at 10,50,75,100 µg/mL ($p < 0.05$), whereas CO-2 and CO-3 within 5-75 µg/mL and CO-4 within 5-100 µg/mL range increased viability ≥100% suggesting proliferation. All CO samples at 25 µg/mL stimulated 3T3 cell migration in Scratch Assay indicating wound healing. CO amounts mainly improved thermal and healing properties of gelatin-based biomaterial. CO-2 was more thermally stable and CO-4 had better influence on cell viability and wound healing than CO-0. Therefore, increased CO ratios, specifically 4:2 and 4:4, G:CO (w:w), in gelatin-based films can be ideal candidates for wound dressing materials.

ARTICLE HISTORY
Received 28 July 2023
Revised Accepted 22 September 2023

KEYWORDS
Coconut oil; gelatin; wound dressing; wound healing; 3T3; cytotoxicity

1. Introduction

Skin covers approximately 15% of body weight and is vulnerable to injuries and external elements such as microorganisms, chemicals and toxins [1,2]. Wound dressings are for immediate use to prevent bleeding and are intended to heal

CONTACT Mehlika Karamanlioglu mkaramanlioglu@gelisim.edu.tr

wounds [3,4]. Since these wound dressings would replace the skin for a while, they should have similar characteristics of the skin and should assist supplements to the wounded skin to restore its structural integrity with its normal function [1]. Therefore, ideal wound dressings should be non-toxic, biocompatible, biodegradable, mechanically improved, elastic, easy to apply; and should inhibit microorganisms, promote wound healing, absorb wound exudates and maintain moisture in the wound environment [2, 5].

Wound dressing materials should also be suitable for the type and place of the wound to be applied on [6]. For instance, less adhesive wound dressings are preferred on burns [7]. Adhesive ones are preferred on extremities and joints that are subjected to movement [8]. Therefore, adhesive wound dressings should both allow the movement of the skin and should not cause any trauma while being removed from the skin surface [9]. Wound dressings can consist of a single material or several materials that include primary and secondary wound dressing materials [9]. The primary wound dressing is the part that contacts the wound and in case there is, the secondary layer is the retention layer [9].

Currently, there are many types of wound dressing materials [5]. Natural polymers, i.e. biopolymers, and some synthetic polymers are preferred as wound dressing materials [10]. Biopolymers have the advantages of biocompatibility, biodegradability, lower antigenicity along with anti-inflammatory, antibacterial and proliferative effects [11]. Gelatin is a protein-based biopolymer formed by cleavage of the collagen, which helps tissue repair and is a component in wound healing [11–13]. Gelatin can be used as a biomaterial and can be an ideal wound dressing material since collagen based wound dressings can absorb wound exudates while retaining moisture in wound site [11,12]. Gelatin is also a hemostatic, bio-adhesive and an inexpensive biomaterial and therefore has been previously studied as a wound dressing and/or wound healing material [14–18]. To improve some properties of gelatin films such as high solubility and low mechanical properties, cross-linking agents and some other materials were incorporated into gelatin films [14,15, 19–22]. Different types of oils have also been added to protein based films, however, mainly for food applications [23–28]. For instance, biodegradable food packaging films were produced from gelatin, coconut oil (CO) and some other oils that were obtained from nutraceutical capsules' waste [25]. Moreover, besides protein, CO was added to carbohydrates such as chitosan but mainly for food packaging applications [29,30].

In this study, different amounts of virgin coconut oil (CO) are added to gelatin-based films for a potential wound dressing material. CO is a plant-based oil that is biocompatible and has antibacterial properties promoting wound healing [31]. Virgin CO is the CO extracted from coconut milk by a wet process [32]. Since it is an edible oil, CO has many applications in food industry [33]. CO is also used in cosmetics for skin moisturizing and skin improvement [33,34]. Although CO has been used in traditional Thai and Indonesian medicine [35,36], emerging medical applications of CO due to its antimicrobial, anti-inflammatory and skin barrier properties have recently been shown in various studies in the literature [34–44]. Moreover, CO has high content of medium chain fatty acids which have many health benefits [38,39, 45,46].

Triglyceride component of CO, lauric acid, is the major saturated fatty acid in CO with 12 carbon atoms in length, therefore, has medium chain fatty acid properties [45, 47]. Lauric acid converts to monolaurin which is involved in immune cell proliferation [36, 48,49]. Monolaurin also has antimicrobial properties since it can disrupt bacterial lipid membrane [37,38, 50,51]. Anti-microbial effects of lauric acid and monolaurin, which are both present in human breast milk as antimicrobial agents, were shown in various studies [38, 40, 52–54]. Monolaurin has also been shown to exhibit sensitivity against some superficial skin infection causing bacteria [55]. When CO was encapsulated in electrospun membranes, antibacterial activity against some bacteria was shown [56].

Wound healing activity of CO was reported when virgin CO was applied topically on young rats as excision wounds were shown to heal faster with higher collagen cross-linking [57]. Other studies showed that, CO increased the healing effect of poly(caprolactone)/gelatin (PCL/Gel) based nanofibers [56, 58]. Micro-emulsions of virgin CO and Tween 80 were incorporated into a microbial polysaccharide, gellan gum, for hydrogel formulations to treat wounds [59]. Similarly, when incorporated to gellan gum films, wound healing effect and non-cytotoxicity of virgin CO was shown on human skin fibroblast cells *in vitro* [31]. In another study, an antibacterial agent, Norfloxacin, was also added to gellan gum with CO for improved antibacterial activity of the films [60]. In another study, when hydrogels of gellan gum contained virgin CO and honey, *in vivo* wound healing was shown to be accelerated [61].

Overall, although CO has many applications, there is limited research when it is incorporated in other biomaterials to be used as wound dressings. Moreover, there are limited comparative studies about the effects of increased CO on wound dressing materials and there is no study to compare all regarding properties to assess the sole effect of CO amounts on a protein-based wound dressing material containing natural components. However, this present research is an extensive comparative study to suggest a primary wound dressing material composed of natural components for minor wounds. Previously, we determined a formulation for a homogenous and continuous gelatin-based film containing a single CO amount and used L929 cell line to show its effect on *in vitro* cell viability and wound healing as a preliminary study [62]. In the present study, we compared the sole influence of increasing CO amounts on gelatin-based biomaterials' properties and on *in vitro* wound healing using 3T3 cell line to suggest the ideal ratios of CO in protein-based wound dressing materials.

2. Materials and methods

2.1. Materials

Powder bovine skin gelatin (G) with average molecular mass of 100 kDa was obtained from Lokman Hekim (Ankara, Turkey). Cold pressed organic virgin coconut oil (CO) was purchased from Naturoil (Çorum, Turkey). Glycerol as a plasticizing agent at 98% reagent grade was obtained from ISOLAB (Eschau, Germany). The emulsifier Tween 80, polysorbate 80, at commercial grade, was obtained from Sigma-Aldrich (Eschau, Germany). Sodium chloride was purchased from Merck (Darmstadt, Germany).

For cell-based experiments, Dulbecco's Modified Eagle Medium/Nutrient Mixture F-12 (DMEM-F12) containing 4.5 g/L of glucose was obtained from Pan Biotech (Germany) and 2,3-bis-(2-methoxy-4-nitro-5- sulfophenyl)-2H-tetrazolium-5 -carboxanilide (XTT), was obtained from Merck (Darmstadt, Germany). The rest of the supplies and chemicals used in cell culture was purchased from Sigma-Aldrich/ Merck (USA), Neofroxx/BioFroxx (Germany), Pan Biotech (Germany), and CAPP (Denmark) and all were of analytical grade.

2.2. Preparation of films

Gelatin films containing CO was prepared by solution casting method adapted from our previous study [62] with various CO amounts. First, film forming solution (FFS) was prepared by dissolving 20% (w/w) gelatin (G) in distilled water at 50 °C on a magnetic stirrer at 1000 rpm for 30 min. Plasticized FFS was obtained by addition of glycerol at 40% (w/w) based on protein content. Then, CO was added into FFS at G:CO ratio of 4:0, 4:2, 4:3, 4:4 (w:w) corresponding to CO-0, CO-2, CO-3, CO-4 films, respectively, in separate beakers. As an emulsifier, 3% (v/w) Tween 80 was added to FFS regardless of the presence of CO. Therefore, CO-0 films contained all the contents of CO-2, CO-3, CO-4 films except for the CO content. When CO ratio was > 4:4 at constant G, films were difficult to handle due to increased oil percentage. Therefore, they were not used for any analyses. CO-2 film without any Tween 80 was also prepared for only optical microscopy analysis. 25 mL of each FFS were cast into glass dishes of 80 × 150 mm and dried at room temperature at a relative humidity (RH) of 40 ± 4% for 2h. Films were conditioned in a controlled environment of *25 °C* ± 4 and 40 ± 4% RH for at least one day prior to any further analyses.

2.3. Optical microscopy

Surface properties of CO-0, CO-2, CO-3, CO-4 films were initially analyzed by optical microscopy (Eschenchau, Germany). Surface of CO-2 film without any Tween 80 was also analyzed. Film samples were placed on a glass slide and the surface analysis was conducted at the magnification of 40x.

2.4. Scanning electron microscopy (SEM)

Surface morphology and cross-section of completely dried films were investigated by SEM (Zeiss EVO® LS 10) at an acceleration voltage of 10 kV. Dried samples were gold–palladium coated prior to examination and analyzed at a magnification of 100-600 times to the original sample size.

2.5. Determination of moisture content; water & physiological saline solution uptake; water & physiological saline solution aging of the films

Moisture content of CO-0, CO-2, CO-3 and CO-4 films containing G:CO at 4:0, 4:2, 4:3, 4:4 (w/w) ratio, respectively, were determined by using the equation given below

in which m_i is the initial mass of samples and $m_{d1}$is the mass of the samples dried at $30\,°C \pm 4$ to a constant mass:

$$\text{Moisture content}(\%) = \frac{m_i - m_{d1}}{m_i} \text{ x } 100 \quad (1)$$

Water & physiological saline solution uptake and water & physiological saline solution aging of the films were determined separately by reported methods [14, 62]. Physiological saline solution of 0.9% concentration was prepared by dissolving sodium chloride in distilled water [63]. In order to determine water & physiological saline solution uptake of films, after recording initial mass of each film (m_i), samples were immersed in each media in separate beakers at room temperature as previously described [14, 62]. Samples were removed periodically after 30, 60, 90, 120, 150 and 180 min, blotted to remove excess water and weighed to determine the final mass of the samples after soaking (m_f) at each time interval as follows:

$$\text{Water / physiological saline solution uptake}(\%) = \frac{m_f - m_i}{m_i} \text{ x } 100 \quad (2)$$

To determine water & physiological saline solution aging of the films, samples were soaked in water and physiological saline solution before dissolution. Then, samples were removed from each media and dried in an environment at a temperature of $30\,°C \pm 4$ to a constant weight (m_{d2}) and aging percentage was calculated using the equation below. Triplicates of samples were used and standard error of the mean was calculated from standard deviation for each measurement.

$$\text{Water / physiological saline solution aging}(\%) = \frac{m_f - m_{d2}}{m_f} \text{ x } 100 \quad (3)$$

2.6. Mechanical properties and thickness

Tensile strength (TS), Young's modulus (YM) and elongation at break (EAB) values of CO-0, CO-2, CO-3, CO-4 samples were evaluated according to ASTM D882 Standard. Prior to testing, thickness of each film was measured with a manual digital micrometer (Mitutoyo, Japan). Zwick Z250 Universal Testing Machine with a cross-head speed of 200 mm/min at 23 ± 2 °C and with a load cell of 1 kN was employed. Triplicates of each film were tested.

2.7. Fourier transform infrared spectroscopy (FTIR)

Perkin Elmer Spectrum 400 FTIR spectrophotometer with attenuated total reflectance (ATR) was used to determine structural interactions in CO-0, CO-2, CO-3 and CO-4 film samples with G:CO at 4:0, 4:2, 4:3, 4:4 (w:w) ratio, respectively. The spectra in the wavenumber range of 650- 4000 cm^{-1} with a resolution of 2 cm^{-1} were collected in 4 scans in transmittance mode.

2.8. Differential scanning calorimetry (DSC)

Thermal analysis of CO-0, CO-2, CO-3 and CO-4 films containing G:CO at 4:0, 4:2, 4:3, 4:4 (w:w) ratio, respectively, were determined by using Perkin Elmer Pyris 1 DSC with heating at 10 °C/min over the temperature range from 10 °C to 250 °C. 5 to 10 mg of each film sample was analyzed in triplicates. Endothermic peaks related to melting temperature of CO, glass transition temperature (T_g) and maximum melt-like transition temperature (T_{max}) of films were determined.

2.9. 3T3 cell culture

The embryonic mouse fibroblast cell line, 3T3, was obtained from Yildiz Technical University, Bioengineering Department and used for *in vitro* cell studies. 3T3 cells were cultured in DMEM-F12 that was supplemented with 4.5 g/L of glucose and pre-mixed with 10% fetal bovine serum (FBS), 100 µg/mL streptomycin and 100 U/mL penicillin in 5% CO_2 incubator at 37 °C. Cells were trypsinized after they reached 80% of confluence. When cells reached 80% of confluence, they were washed with PBS for 3 times to remove the FBS residues. Then cells were dissociated with Trypsin EDTA and transferred into sterile Falcon Tubes to centrifuge at 1200 rpm for 10 min. Following the centrifugation, a-2µL-of cell suspension was stained with Trypan Blue prior to counting with a hemocytometer (Marienfeld, Germany). After cell counting, cells were seeded at a density of $1x10^4$ cells/well into 96-well plates and incubated for 24 h, for XTT Assay. T25 flasks were used to seed and culture the cells which were kept until further use.

2.10. XTT assay for cytotoxicity and cell viability assessment

The influence of CO-0, CO-2, CO-3, CO-4 films on viability of 3T3 cell line was determined by XTT assay which is a commonly used colorimetric assay for *in vitro* quantification of cellular proliferation, viability, and cytotoxicity [64]. In order to determine the non-toxic concentrations of film samples, a method that we previously used was employed [62]. Prior to XTT Assay, 3T3 cells at a density of 1×10^4 were plated in a 96-well plate (TPP, Zurich, Switzerland) containing DMEM-F12 with 10% FBS as growth medium; and incubated overnight [65]. When 3T3 cells were attached to the surface of cell culture plate [65], they were washed with PBS twice.

Each film sample was melted in water bath at 45 °C in flasks prior to XTT Assay. Liquid samples were cooled down to 37 °C and then were added into phenol red containing DMEM-F12 medium with no FBS at a final concentration of 5, 10, 15, 25, 50, 75 and 100 µg/mL in six replicates. After 3T3 cells were washed with PBS twice, each liquid film sample at a certain concentration was added to the adhered 3T3 cells in wells and incubated for 24 h at 37 °C and 5% CO_2 in a culture hood. Then, XTT solution was added into each well and incubated for 4 h. Cell viability was measured at 570 nm wavelength by using ELISA microplate reader (Fluoroskan Ascent, Thermo Lab systems, Finland). In this assay, 100% viable cells were used as the control which was 3T3 cells incubated with DMEM-F12 basal medium containing FBS without any film sample.

2.11. Scratch assay for wound healing characterization

The wound healing effect of CO-0, CO-2, CO-3, CO-4 films was determined on 3T3 cell line by scratch assay [66]. Initially, cells at a density of 6 x 10^5 were seeded into 24-well plate with DMEM-F12 containing 10% FBS as growth medium. After incubation for 24 h, cells were washed with PBS twice and DMEM-F12 without FBS was added for starvation overnight which is necessary to eliminate the proliferation tendency of the cells. Next day, a straight cell-free gap, i.e. scratch, was created in cell monolayer by direct manipulation [66]. Prior to the scratch assay, each film was melted at 45 °C in a water bath and turned into liquid form; and mixed with DMEM-F12 without FBS to give a final concentration of 5, 10, 15, 25, 50, 75, 100 µg/mL. After the scratch formation, wells were washed gently and liquid samples of CO-0, CO-2, CO-3 and CO-4 at each concentration were added into each well for a 24-h-incubation with 3T3 cells at 37 °C and 5% CO_2. Triplicates of each film sample at each concentration were used. 3T3 cell line incubated with DMEM-F12 basal medium containing neither CO nor FBS was used as a negative control. 3T3 cell line incubated with DMEM-F12 basal medium containing 5% FBS without any CO was used as a positive control. All cell cultures and scratch formation were monitored qualitatively under a fluorescence inverted biological microscope (INV100-FL, Bell) at 100x magnification during the incubation of cells.

2.12. Statistical analyses

IBM SPSS Statistics 24 Version was used for the analysis of variance (one-way ANOVA) and for the Tukey's HSD (honestly significant difference) tests to assess statistical significance of any difference in mechanical properties and also thickness of CO-0, CO-2, CO-3 and CO-4 films. One-way ANOVA and Tukey's HSD were also used to evaluate statistical significance of any difference between the control group of 100% viable cells and the viability of cell lines treated with CO-0, CO-2, CO-3 and CO-4 film samples which were also compared among each other. Significance threshold was set at P value < 0.05. Results are shown with mean ± standard error of the mean which is calculated from standard deviation.

3. Results and discussion

3.1. Formation and physical appearance of films

Flexible, homogenous and bio-adhesive CO-0, CO-2, CO-3, CO-4 films at 4:0, 4:2, 4:3, 4:4 (w:w) G:CO ratio, respectively, were obtained by solution casting method. Mechanically strong and elastic wound dressing biomaterials are preferred for a long-term application on the skin surface [2, 15]. Since neat gelatin films have poor mechanical properties, gelatin films are often plasticized for wound dressing applications; and due to its miscibility with gelatin, glycerol is often preferred as a plasticizing agent to improve flexibility of the films [28, 67]. Therefore, gelatin was plasticized with glycerol in this study.

CO is immiscible with most polymers solution due to interfacial tension [31]. Therefore, homogenous CO distribution was obtained when FFS contained 3% (v/w) Tween 80 as an emulsifier. Tween 80 is a non-ionic surfactant with a wide range of applications such as in food industry and cosmetics due to its low order toxicity [59, 68]. Tween 80 was also added to control films, CO-0, in order to assess the sole effect of various CO amounts in gelatin-based films. CO is solid below the room temperature, however, in this study since CO was emulsified, temperature of the environment did not influence homogeneity of the cast films.

Each film is shown in Figure 1 and the transparency of films can be assessed by the dark line drawn in the background. When a transparent dressing is used, wound healing can be observed without removing the dressing material from wound site [69]. Transparent and glossy films were obtained with CO-0 films and slightly less transparent and matte films were obtained when increasing amount of CO was incorporated. Since the dark line could still be observed behind the CO incorporated films, increasing CO up to 4:4, G:CO ratio did not decrease transparency of the films.

In our previous study, CO incorporated gelatin film without Tween 80 were shown to be heterogeneous and partly opaque [62]. In this study, CO-2 film without Tween 80 (image not shown) was only used for optical microscopy and no further analysis was conducted due to the brittle and slippery nature of the films.

3.2. Surface analysis of films

Surface of films were initially analyzed by optical microscopy at 40x magnification. Since proteins are known to form continuous matrix [67], continuous plasticized gelatin matrix with Tween 80 was observed when no CO was incorporated (Figure 2a). When CO was added to films, oil droplets in gelatin matrix was observed. In order to demonstrate CO droplets in gelatin without the influence of Tween 80, surface analysis of CO-2 film with no Tween 80 was also conducted by optical microscopy (Figure 2b). Plasticized gelatin matrix was covered by non-homogenous distribution of oil droplets. Previously, oil incorporation to hydrophilic phase of dressing materials is reported to decrease dispersion of oil droplets in the matrix [70,71]. However, when Tween 80 was added, more homogenous film surface was observed at the same CO concentration (Figure 2c). Therefore, the surfactant incorporation caused a better droplet dispersion in gelatin matrix and also reduced size of oil droplets. In CO-2

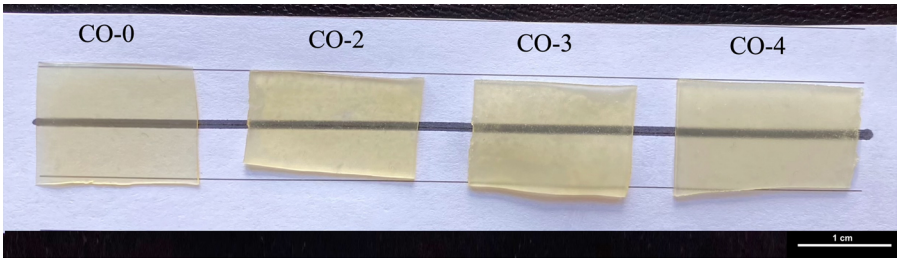

Figure 1. Photograph of CO-0, CO-2, CO-3, CO-4 films at G:CO ratio of 4:0, 4:2, 4:3, 4:4 (w:w). Scale bar represents 1 cm.

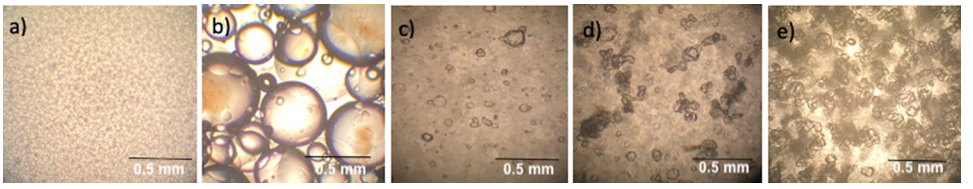

Figure 2. Optical microscope images of a) CO-0 b) CO-2 without Tween 80 c) CO-2 d) CO-3 e) CO-4 films. Scale bar represents 0.5 mm.

films containing Tween 80, single oil droplets were dispersed on the surface of films. However, as the ratio of CO increased in the films, oil droplets formed clusters observed as dark spots on the surface of CO-3 and CO-4 (Figure 2d, e, respectively). Therefore, when G:CO ratio was 4:2, CO dispersion within the matrix was more uniform. Similarly in another study, intermediate amounts of essential oils dispersed more efficiently in sodium alginate films [71].

Scanning Electron Microcopy (SEM) was also used to analyze surface and also cross-section of dried CO-0, CO-2, CO-3, CO-4 films (Figure 3). CO-0 had homogenous, more cohesive and smoother surface compared to CO incorporated films due to the ordered phase of gelatin network (Figure 3a) [28]. The surface of CO incorporated films had rough surfaces due to the oil droplets (Figure 3b, c, d). In literature, surface roughness and hydrophobicity due to the oil content were shown to influence cell behavior [31, 72]. The presence of the oil at the appropriate amount was also determined to induce cell attachment [72]. Different oil contents caused rougher surfaces in protein-based films in the literature as well [26–28, 62]. Olive oil emulsified gelatin films also had caves, pores and oil droplets in the film microstructure [73]. Phase separation was observed on the surface of specifically CO-2 films. Due to the hydrophobicity of oil, CO droplets were separated from the aqueous phase forming an immiscible phase since hydrophobic content was reported to disrupt uniformity of films [23, 27,28, 62, 74]. Although Tween 80 was an effective surfactant as observed visually (Figure 1) and by light microscopy (Figure 2b, c); oil phase may have caused creaming since oil migrated to the film surface during casting of the films and enhanced phase separation [26, 28]. Similarly in another study, oil content caused phase separation on the upper surface of gelatin films despite the chemical and mechanical homogenization of oil [28]. When rosemary essential oil (REO) was incorporated to gelatin based films for food packaging applications, oil droplets were observed throughout the film matrix due to the hydrophobicity of REO causing an immiscible phase despite the addition of a surfactant [27]. CO-3 films had a rougher surface due to formation of irregular and big pores of ~20-100 µm in size. SEM images of CO-4 films showed not only more but bigger oil droplets since clusters of oil droplets collapsed together as observed *via* optical microscopy as well (Figure 2e). However, no pores were observed on CO-4 films since clusters of CO droplets were dispersed throughout the surface.

Cross-section of CO-0 was smoother than those incorporated with CO. Heterogeneous and rough cross sections with discontinuity were observed when films contained increasing CO content. Cross section of CO-2 film was smoother than CO-3 and CO-4, although some irregularities were observed throughout the

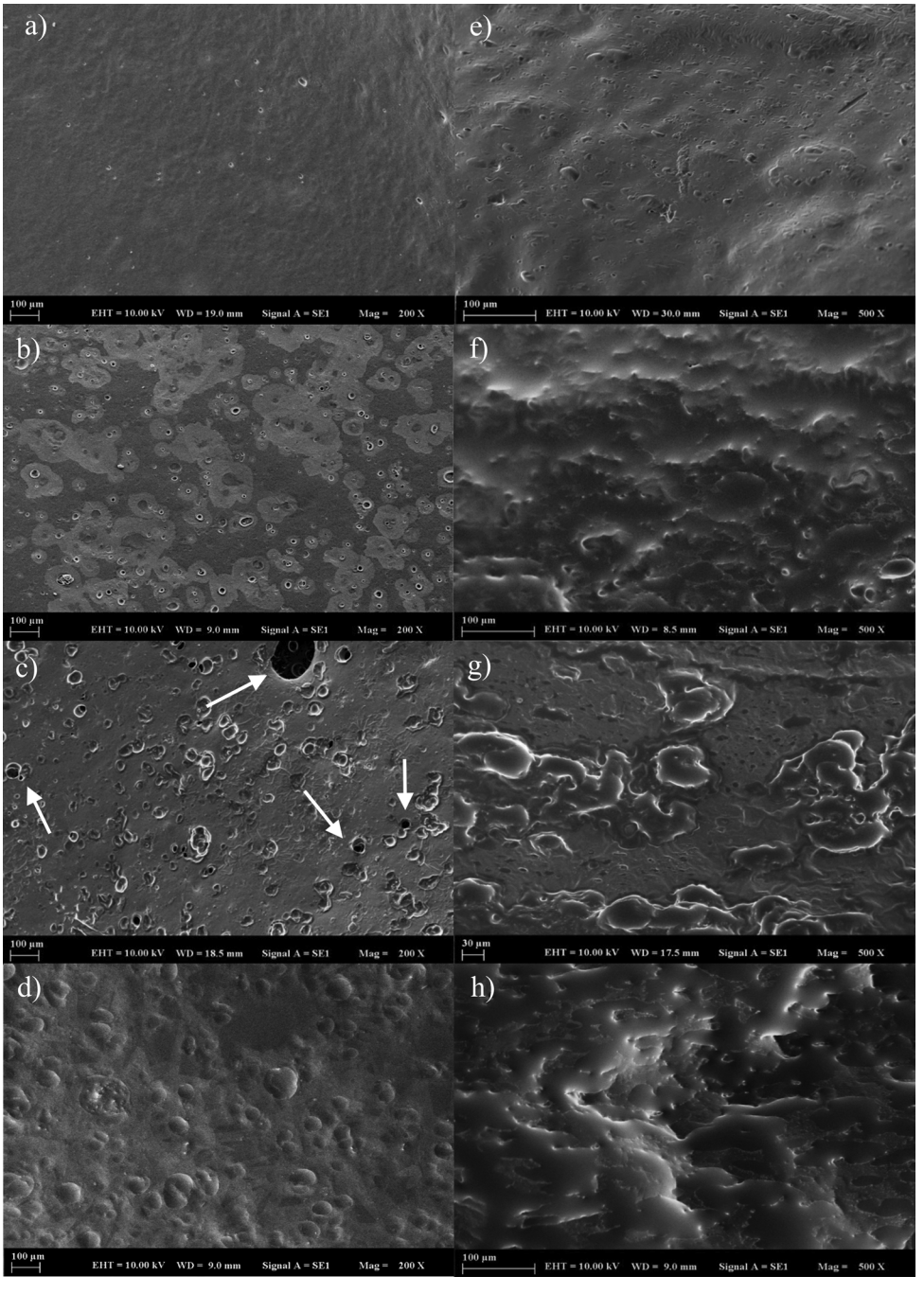

Figure 3. SEM images of surface of a) CO-0 b) CO-2 c) CO-3 d) CO-4 films; and cross-section of e) CO-0 f) CO-2 g) CO-3 h) CO-4 films. Pores >20 µm in diameter are indicated by arrows.

cross section of the film. CO droplets localized in film matrix was more obvious in SEM images of CO-3 films. Oil droplets were dispersed throughout the matrix and caused roughness in the cross-section of CO-3 films similar to another study where

cross section of gelatin films exhibited roughness due to the inclusion of oil droplets [28]. Since the ratio of CO increased in the films, CO droplets were embedded throughout the matrix of CO-4 films and no cracks and pores were observed similar to the surface of the films. Increased amount of CO in CO-4 films may have acted like a plasticizer and prevented and/or filled the formation of cracks and pores as another study added CO to gellan gum hydrogels as a plasticizer to improve the mechanical properties of films such as flexibility [59].

3.3. Moisture content, water & physiological saline solution uptake and aging of the films

Increasing amount of CO decreased moisture content of films due to hydrophobic nature of CO. Moisture content percentage of CO-0 was reduced by more than half when compared to CO-4 (Table 1).

Water and physiological saline solution uptake of films were determined since high water and saline solution uptake percentages are ideal for wound dressing materials to remove exudates from open wounds [9, 14, 75]. Water and saline solution uptake of all films increased over time, however, increasing amount of CO decreased water and saline uptake capacity of films (Figure 4a, b, respectively).

Since gelatin is a hydrophilic biopolymer, CO-0 had the highest percentage of water uptake, ≃305%, before starting to dissolve after 150 min in water, therefore, the mass of the film decreased causing decreased water uptake at the 180th min (Figure 4a). In the presence of CO, water uptake percentages of CO-2, CO-3, CO-4 films were ≃186%, 184%, 152%, respectively, after 150 min in water and then they all became saturated with a steady water uptake. Unlike CO-0, CO incorporated films were intact after 180 min in water since oil content of films retarded dissolution of films in water. In our preliminary study, gelatin film also dissolved faster than the CO-incorporated gelatin film [62].

Similar trend was observed in saline solution uptake of films as CO-0 films had the highest uptake percentage of ≃291%, whereas CO-2, CO-3, CO-4 films had ≃258%, 233% and 149% saline solution uptake capacity, respectively, after 180 min in saline solution before dissolving (Figure 4b). Both water and saline solution uptake percentages of CO-4 films were the lowest and almost half of the capacity of CO-0 films due to the increased amount of hydrophobic oil content. However, since both percentages were still higher than 100%, increasing CO content did not prevent water and saline solution uptake capacity of any CO containing films including CO-4.

Phase separation was observed by SEM especially in CO-2 films which may have caused more water to penetrate into the matrix contacting the hydrophilic content of

Table 1. Moisture content of CO-0, CO-2, CO-3, CO-4 films.

Samples	Moisture content (%)
CO-0	50 ± 0.1
CO-2	44.8 ± 2.7
CO-3	31.6 ± 1.7
CO-4	20 ± 5

Data shows the mean of 3 replicates for each sample ± standard error of the mean.

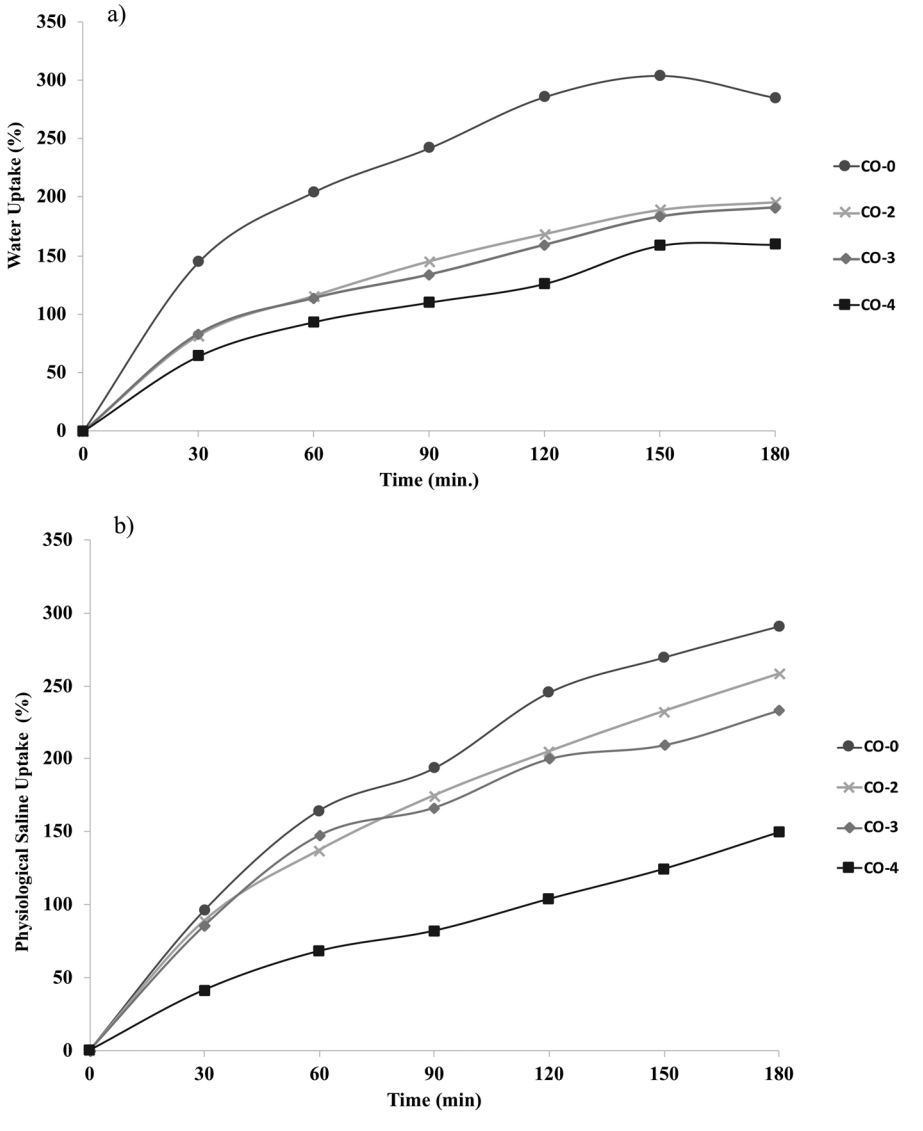

Figure 4. Comparison of a) water uptake b) physiological saline solution uptake of CO-0, CO-2, CO-3, CO-4 films.

Table 2. Water and physiological saline solution aging of CO-0, CO-2, CO-3, CO-4 films.

Samples	Water aging (%)	Physiological saline solution aging (%)
CO-0	90.1 ± 0.1	87.3 ± 0.3
CO-2	84.2 ± 0.5	85.1 ± 0.1
CO-3	80.4 ± 0.1	84.1 ± 0.4
CO-4	76.0 ± 0.3	73.6 ± 1.8

Data shows the mean of 3 replicates for each sample ± standard error of the mean.

films [76] and therefore, increased water and saline solution uptake of films were recorded despite the hydrophobic oil content.

Water aging analysis showed that CO-0 films had the highest percentage of water aging, due to the higher water uptake compared to films with CO (Table 2). Similarly, saline solution aging of CO-0 films was higher than all CO containing films (Table 2). Due to hydrophobicity, increasing oil content decreased water and saline solution aging of films as aging of CO-4 films was about 14% less than aging of CO-0 films in both media. Neat gelatin dissolves fast in aqueous media affecting aging of the films; and therefore, solubility of gelatin has to be improved to be used as a wound dressing material [21]. Since low water aging percentages are ideal for wound dressing materials [14], increasing CO content improved aging of the films. In other studies, crosslinking agents were incorporated to gelatin-based films to decrease solubility which affects water aging percentages [21]. Apart from the influence of the hydrophobic content, gelatin amount may affect the solubility of the films. Since gelatin is a hydrophilic biomaterial, gelatin wound dressing materials containing 10% (w/w) gelatin dissolved in water under 10 min at room temperature and/or at 32 °C in literature [14,15]. It is also reported that increasing gelatin concentration in FFS decreased solubility of gellan/gelatin composite films [77]. Therefore, in this study, since the films contained 20% (w/w) gelatin with Tween 80 and glycerol in the FFS, samples retained in water longer than films containing lower amount of gelatin used in other studies [14,15]. Overall, 20% (w/w) gelatin and increasing CO improved durability of the gelatin-based films.

3.4. Mechanical properties and thickness

In order to measure the effect of CO on thickness and mechanical properties of gelatin- based wound dressing materials, thickness, tensile strength (TS), Young's modulus (YM) and elongation at break (EAB) of films were measured (Table 3).

Thickness values of the films were measured prior to mechanical testing and used in mechanical testing as well. As shown in Table 3, thickness of the films increased with increasing CO and thickness of CO-4 was significantly more than CO-0 ($p < 0.05$). Similarly, higher oil content in gelatin films increased thickness of the films due to the increased solid content [25,26].

TS of CO incorporated films significantly decreased with increasing CO amount ($p < 0.05$); and YM also decreased in CO-2 and CO-3 ($p > 0.05$) and CO-4 ($p < 0.05$) when compared to CO-0 (Table 1). Microstructure of the films might be the main influence on the mechanical properties of the films since SEM analysis showed that

Table 3. Thickness, tensile strength (TS), Young's modulus (YM) and elongation at break (EAB) of CO-0, CO-2, CO-3, CO-4 films.

Samples	Thickness (mm)	TS (MPa)	YM (MPa)	EAB (%)
CO-0	0.55 ± 0.02^{a}	6.70 ± 0.89^{a}	25.26 ± 7.84^{a}	177.06 ± 20.99^{a}
CO-2	0.65 ± 0.07^{ab}	4.00 ± 0.15^{b}	7.83 ± 1.39^{ab}	207.50 ± 9.67^{a}
CO-3	0.65 ± 0.08^{ab}	2.83 ± 0.08^{b}	7.40 ± 1.96^{ab}	152.33 ± 7.79^{a}
CO-4	0.80 ± 0.03^{b}	2.43 ± 0.12^{b}	4.53 ± 1.04^{b}	178.82 ± 4.34^{a}

Data shows the mean of 3 replicates for each sample ± standard error of the mean. Different superscripts in the same column show the significant difference ($p < 0.05$).

CO caused rough and heterogeneous surfaces (Figure 3). Similarly, in other studies, introduction of oil content into protein films caused a heterogeneous structure and discontinuities in the matrix which caused significant TS decrease of the films [24, 26, 78]. Moreover, high amount of CO droplets in poly(caprolactone)/gelatin nanofibers was claimed to act as stress concentration zones to decrease TS [56]. YM decrease was observed due to the addition of oil content into the protein films as well [21, 31, 60, 78]. CO incorporation to gellan gum films also caused rough cross-sections and thereby, significant TS and YM reduction was measured [60]. Flexibility, reflected by EAB, is an important feature of wound dressing materials since they need to adapt to motion and to uneven surfaces on the body [2, 15, 31]. In this study, CO content did not significantly increase in EAB of the films, however, CO-2 films' stretching capacity was more than CO-0 and other CO incorporated films' capacity. Previously, oil incorporation to protein films was shown to increase EAB due to plasticizing effect of the oil with TS decrease [21, 26, 78–80]. Specifically, when CO was used in gellan gum films, it increased elasticity of the films due to the plasticizing effect of CO [31].

Overall, CO-2 had the highest TS, YM and EAB in CO incorporated films since it had a smoother surface and cross-section especially compared to CO-3 due to the lack of pores bigger than 20 µm. CO-4 had the lowest TS and YM among CO films and had significant TS and YM decrease compared to CO-0 ($p < 0.05$) since oil incorporation at certain amounts is claimed to reduce polymer interactions decreasing rigidity accompanied by an increase in elasticity [79,80]. Similarly, increased CO may have shown a plasticizing effect since EAB of CO-4 was improved when compared to CO-3 films (Table 3). Microstructure of CO-3 showed pores on the surface of the films (Figure 3) which decreased the EAB, whereas, no pores were observed on CO-4 due to increased oil droplets covering the surface of the films and possibly filling the pores as a plasticizer (Figure 3).

3.5. FTIR

FTIR was used to compare structural interactions within the matrix of gelatin-based films when contained increasing amounts of CO. Since gelatin is a protein, main vibration peaks of protein were observed in all spectra of films (Figure 5a). Amide-A band of gelatin, a main peak observed in overlay spectra of films, is reported to be at ~3400 cm^{-1} corresponding to N–H stretching vibration, however, when NH group of peptide chain is involved in hydrogen bonding, amide-A band is reported to shift to lower wavelengths (Figure 5a) [81–83]. In CO-0 films amid-A band was observed at 3318 cm^{-1}, however, it shifted to a lower frequency of 3292 cm^{-1} in all CO incorporated films. Since shift of amide-A band to lower frequency represents presence of hydrogen bonding between protein molecules [28, 84], protein-protein interaction increased when films contained CO. In accordance with this, amplitude of amide-A peak of films decreased as CO increased which is an indication of decreasing amount of free-amino groups (Figure 5b) [83]. Similarly, in other studies amide-A band shifted to lower wavelengths when certain concentrations of essential oils were added to protein based films due to hydrogen bonding [24, 26].

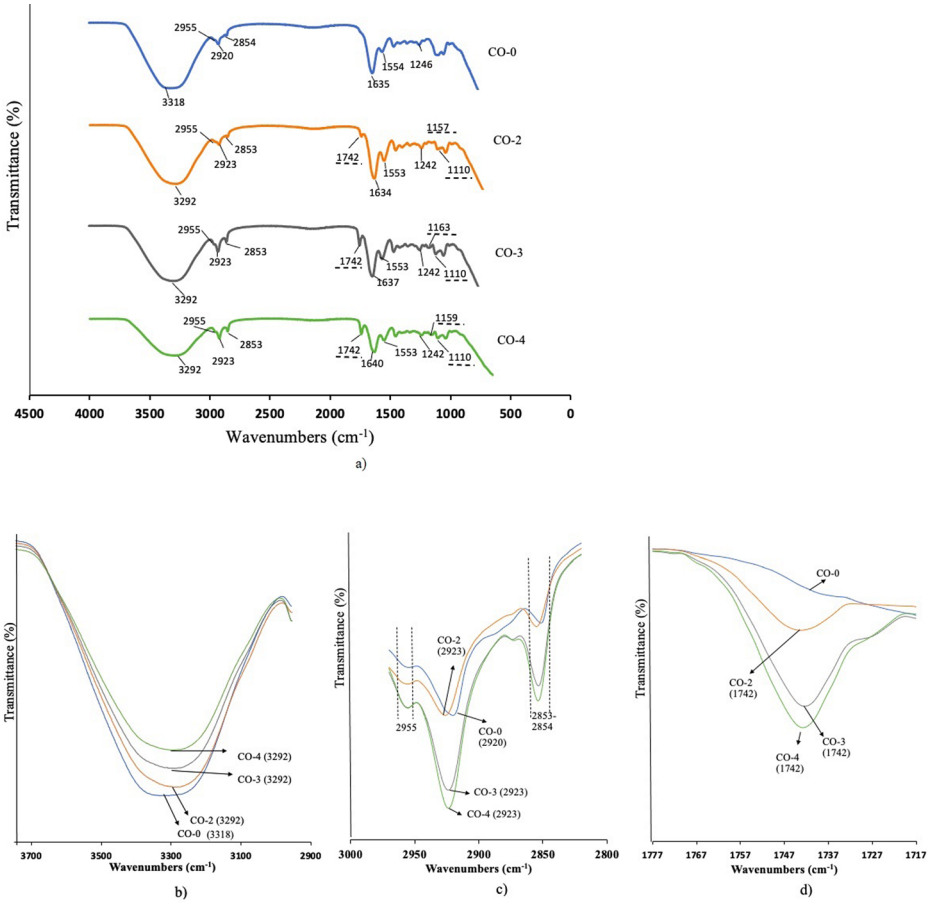

Figure 5. The FTIR of CO-0, CO-2, CO-3 and CO-4 films: a) overlay spectra of films at the whole range of 4000-650 cm^{-1}. Underlined wavenumbers correspond to peaks observed in only CO incorporated films b) Overlapping spectra at 3700-2900 cm^{-1} c) overlapping spectra at 3000-2800 cm^{-1} d) overlapping spectra at 1777-1717 cm^{-1}.

Another main peak was amide-I band of gelatin showing C=O stretching and was situated at 1635 cm^{-1} and 1634 cm^{-1} in CO-0 and CO-2, respectively, however shifted to higher frequencies of 1637 and 1640 in CO-3 and CO-4, respectively (Figure 5a) [83, 85]. Lower frequency of amide-I band observed in CO-2 films corresponds to more hydrogen bonding of C=O groups of gelatin [83] which may have caused CO-2 to have the highest TS and YM properties among CO incorporated films.

The peak corresponding to amide-B band of gelatin was situated at 2955 cm^{-1} in all samples and its amplitude increased as CO ratio increased in the samples (Figure 5c). Amide-II and amide-III peaks were previously reported to be at 1548-1565 cm^{-1} and at 1240 cm^{-1}, respectively, depending on the gelatin type [85,86]. In this study, amide-II and amide-III bands of CO-0 films were situated at the wavelengths of 1554 cm^{-1} and 1246 cm^{-1}, respectively. Amide-II and amide-III bands shifted to 1553 cm^{-1} and 1242 cm^{-1} in all CO incorporated films (Figure 5a). Wavelengths shifts as well as amplitude differences upon incorporation of CO can

be attributed to the interactions between functional groups of oil and protein as suggested by other studies involving protein-based films containing different oils [24, 26, 62]. These interactions in the presence of CO may have contributed to discontinuities in the gelatin matrix, thereby reducing the TS and YM of the films [26, 79].

The peaks situated approximately at 2920 cm^{-1} and 2853 cm^{-1} correspond to asymmetric and symmetric C-H stretching, respectively and were previously identified in virgin CO [46]. Although these peaks were present in all samples, their amplitude increased as CO ratio in the films increased (Figure 5c). Likewise, in another study, when olive oil was incorporated to gelatin films, C-H stretching peaks appeared in oil olive samples with a higher amplitude [87].

Some peaks appeared only when films contained CO since hydrophobic CO formed an immiscible emulsified phase in gelatin films as observed by SEM (Figure 3). Likewise, in another study when olive oil formed an immiscible phase in gelatin films, distinctive peaks of olive oil were observed [87]. FTIR spectra of animal and vegetable fats/oils are reported to be similar due to the presence of triglycerides with some differences in amplitude and exact frequency of wavelengths due to the length and unsaturation degree of acyls in triglycerides [88–90]. One of the significant bands identified from triglycerides of lipids/fats is situated at 1742 $cm^{-1}$and is assigned to stretching vibration mode of ester carbonyl group [90,91]. This peak was observed in only CO incorporated films due to the triglyceride component of CO [47] and therefore, the amplitude of this peak increased with increasing amount of CO (Figure 5d). Characteristic virgin CO peaks were reported to be situated at 1109 and 1151 cm^{-1} [46]. Likewise, the peaks within 1157-1163 cm^{-1} range and at 1110 cm^{-1}

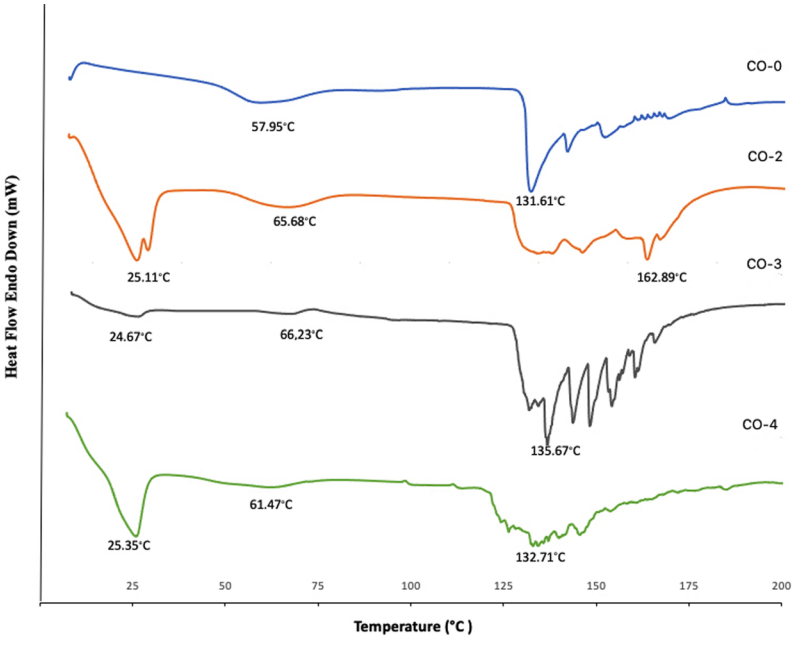

Figure 6. DSC thermograms of CO-0, CO-2, CO-3 and CO-4 films.

corresponding to stretching vibration mode of C–O ester groups of oil were observed only in samples containing CO (Figure 5a) [90, 92].

3.6. DSC

Influence of various CO amounts on thermal transitions of gelatin films upon thermal change were determined by comparing thermogram of CO-0 with thermograms of CO-2, CO-3 and CO-4 films containing increasing amounts of CO (Figure 6). Endothermic peaks at ~25 °C were related to the melting of CO in the films as ~25 °C is reported to be the melting temperature (T_m) of CO [46] and were only observed in CO incorporated films due to the medium-chain fatty acid, lauric acid, content of CO. Medium-chain fatty acids have low melting points and therefore, CO is in liquid phase at room temperature when not emulsified in any material [47].

An endothermic peak was observed in all films at the temperature range of 57-67 °C corresponding to glass transition temperature (T_g) which is related to the amorphous structure of gelatin based films [83]. The lowest T_g was observed in CO-0 as lower T_g indicates lower thermal stability of CO-0 [83]. Moisture content of CO-0 films were the highest (Table 1) and more moisture content percentage causes a more amorphous structure which decreases T_g [93]. Increased and broader T_g values were observed in CO containing samples. Incorporation of CO reduced the moisture content to < 45% (Table 1) and increased T_g of CO-2, CO-3 and CO-4 films.

In gelatin based films, endothermic transition succeeding T_g was determined to be the temperature that mainly dissociates highly structured, i.e. crystalline, regions of gelatin corresponding to melt-like transition of gelatin in the films [26, 67, 83, 94]. Moreover, the endothermic transition after T_g is also attributed to disruption of other ordered molecular structures [83]. In this study, many endothermic peaks with broad ranges were observed which may be related to dissociation of gelatin and other ordered molecular structures corresponding to melting of the films. Multiple peaks can also be attributed to presence of crystals with various sizes in the films since minor peaks preceding or succeeding the main peak during melting was attributed to melting and recrystallization of different sizes and types of crystalline regions [95]. Similarly, in another study increasing amount of CO in gellan gum films yielded broader endothermic peaks with a wide range as melting point of films [31]. Therefore, it is reported that CO incorporation in the films affected crystallization of the films and improved thermal properties [31]. In this study, maximum endothermic peak of melt-like transition (T_{max}) of CO incorporated films, especially CO-2, were higher than CO-0 (Figure 6). Since CO-0 films had the lowest T_g and T_{max}, CO-0 films exhibited less thermal stability than CO incorporated films. FTIR showed that amide-A was situated at a lower frequency in CO containing films indicating more hydrogen bonding which may have caused a more ordered molecular structure, thereby increasing their T_{max}.

Among CO-incorporated films, CO-2 had the highest T_{max} at ~163 °C whereas T_{max} of CO-3 and CO-4 films were observed at ~136 and ~133 °C, respectively. Amide-I band was at a lower frequency in CO-2 films showing more hydrogen bonding of

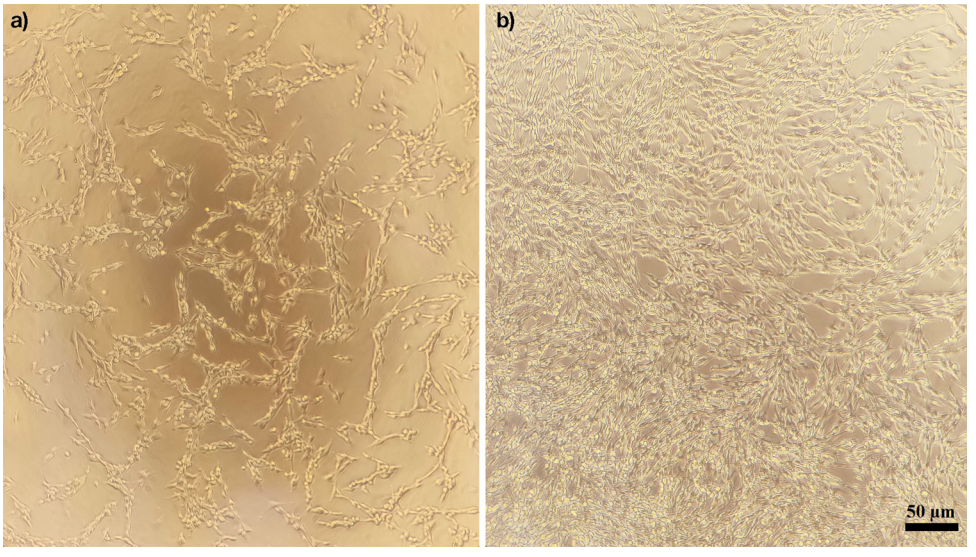

Figure 7. Microscopic image of 3T3 cell line after Passage on a) day 3 and b) day 7, 100x.

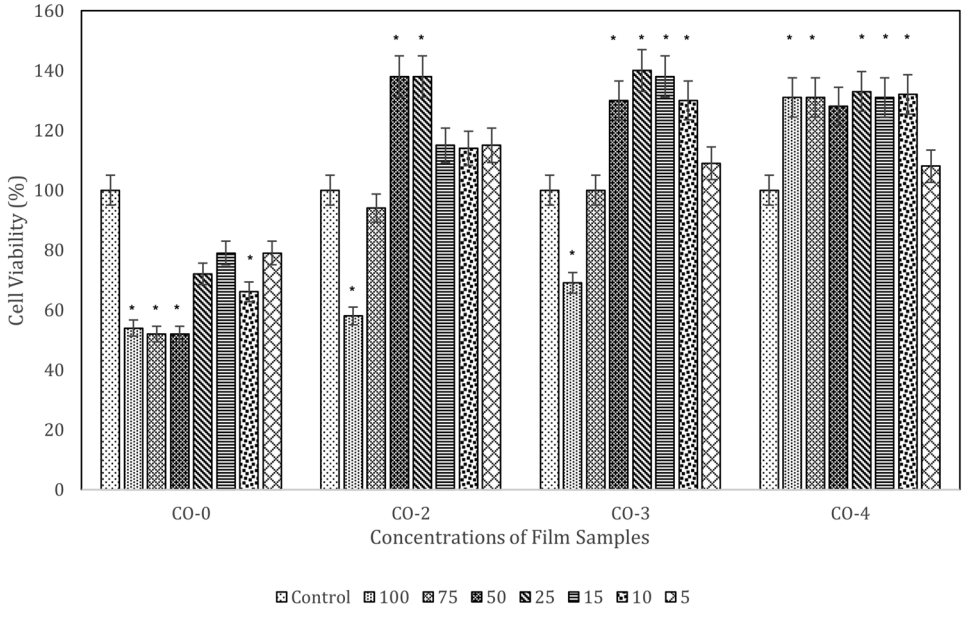

Figure 8. Effect of CO-0, CO-2, CO-3 and CO-4 film samples at 7 different concentrations within a range of 5 -100 µg/mL. Control is the 100% viable 3T3 cell culture incubated in basal medium containing FBS. Concentration of each film significantly different from the control is shown at the top of the bars ($^*p < 0.05$).

C=O which may also have contributed to a higher T_{max} of CO-2 films having a higher extent of molecular order. Therefore, when G:CO ratio was 4:2, more thermally stable films, which also had more ideal mechanical properties among CO films, were obtained.

3.7. 3T3 cell culture

Fibroblast cell lines, such as 3T3 mouse embryo fibroblast cell line, have been used for biological evaluation of biomaterials such as for cytotoxicity assays and for wound healing assays in skin engineering research [96–103]. In this study, 3T3 cells were incubated in a humidified culture hood and were observed daily by an inverted microscope. As seen in Figure 7, adherent cells reached confluence at day 7 and showed intact characteristics; therefore, they were further prepared to be used in cell-based assays.

3.8. Cell viability

Non-toxic concentrations of CO-0, CO-2, CO-3 and CO-4 liquefied film samples at 7 different concentrations within the range of 5-100 µg/mL were evaluated by XTT Assay (Figure 8). The effect of increasing CO concentration on 3T3 cell growth was assessed as percent cell viability. Cells incubated in basal medium containing FBS without any CO were regarded as 100% viable and used as a control group of cell cultures. The influence of each liquefied film within the range of 5-100 µg/mL concentration on cell viability was compared with the 100% viable control group. In order to determine the effect of CO, the viability of cells incubated with CO-2, CO-3 and CO-4 samples were compared with the viability of cells incubated with CO-0 samples. Moreover, viability within the cells incubated with CO-2, CO-3 and CO-4 samples were compared with each other to determine the effect of increasing amount of CO.

When compared with 100% viable control group, cell viability results showed that CO-0 samples decreased 3T3 cell viability especially at 10, 50, 75 and 100 µg/mL significantly ($p < 0.05$) (Figure 8). However, CO incorporated films generally maintained the viability of 3T3 cell culture. CO-2 and CO-3 samples decreased viability only at 100 µg/mL significantly ($p < 0.05$). Viability of cells treated with 5, 10, 15 and 75 µg/mL of CO-2 samples were similar with the 100% viable control group ($p > 0.05$) and viability was significantly increased when treated with 25 and 50 µg/mL of CO-2 samples ($p < 0.05$). CO-3 samples at 10, 15, 25, 50 µg/mL; and CO-4 samples at 10, 15, 25, 75, 100 µg/mL significantly increased 3T3 viability as well ($p < 0.05$). This significant increase in viability only in the presence of CO shows the potential proliferative effect of CO in gelatin based films since increased number of daughter cells indicates cell proliferation [104,105] which is in accordance with a previous study that determined CO enhanced fibroblast proliferation [57]. Our preliminary study also showed an increase of L929 cell viability only when gelatin sample contained CO [62]. In another study, certain CO amounts in

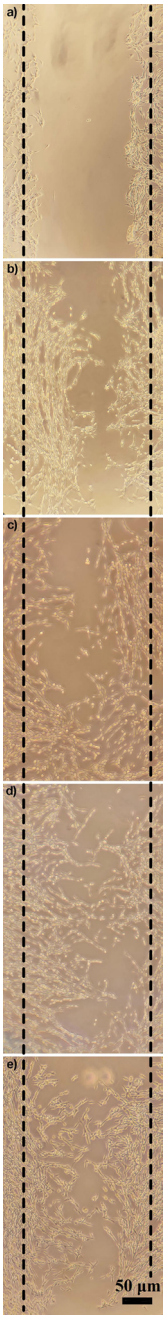

Figure 9. Microscopic images to evaluate Scratch assay-wound closure on 3T3 cell lines incubated with a) neither FBS nor CO as negative control b) 5% FBS without any CO as positive control c) 25 µg/mL CO-2 d) 25 µg/mL CO-3 e) 25 µg/mL of CO-4 for 24 h, 100x.

nanofiber scaffolds was shown to increase viability more than 100% due to better cell attachment and proliferation [56].

When viability within CO-2, CO-3 and CO-4 samples were compared, it was observed that increasing amount of CO in films increased viability percentage of cells. When incubated with CO-4 samples at every concentration within 5-100 µg/mL, viability of cells was either similar to or significantly more than 100% viable cells, whereas CO-2 and CO-3 samples at 100 µg/ml decreased 3T3 cell viability significantly ($p < 0.05$). Therefore, CO-4 samples improved viability and proliferation of the cells more. Biocompatibility and non-cytotoxicity of virgin CO or compounds of CO on fibroblast cells *via* cell viability were also demonstrated in other studies as well [31, 106].

3.9. In vitro wound healing

In tissue engineering, the scratch-wound assay provides important data on the effects of studied materials on cell migration [107,108]. This assay is one of the simple and inexpensive methods mimicking *in vivo* cell proliferation and migration by using *in vitro* reproducible means [101, 108]. In this assay, after forming a scratch, i.e. wound, in monolayer cell culture, directional cell migration towards the scratch to demonstrate healing was observed *via* microscopy during the incubation period [66, 99, 108]. Scratch Assay with fibroblast cell lines was also previously employed in other studies as a wound healing assay [97–99, 101, 109]. Wound healing activity of some plant extracts was determined effectively by scratch assay using 3T3 fibroblast cells [101]. In wound healing process, fibroblast cells are essential since they migrate to wound area for granulation, for fibroblast growth factor (FGF) secretion and eventually for reconstitution of the integrity of the skin [110,111]. FGF is a cytokine secreted by fibroblast cells that take place in healing process [100, 112].

In our study, liquefied samples of all films were mixed with the cell culture medium to give a final concentration within the range of 5-100 µg/mL; and then each different concentration of samples was incubated for 24 h with healthy and intact 3T3 cells which were previously adhered to the cell culture dishes. Microscopic images of the scratch on confluent 3T3 cells were observed *via* inverted microscopy and captured to determine basic cell migration for closure of injury during the incubation period. The improvement of healing was compared against a negative control in which 3T3 cell line was incubated with DMEM-F12 basal medium for 24 h and no closure of scratch was observed (Figure 9a). Moreover, 3T3 cell line incubated with DMEM-F12 basal medium containing 5% FBS was used as a positive control group in which closure of scratch was observed after 24 h indicating healing (Figure 9b).

Results showed that incubating cells with CO-0 samples at any concentration caused detachment of 3T3 cells from the bottom of the microplate wells as a result of deterioration of cells. It was previously reported that cells lose their adherence due to cell death [113]. Since XTT Assay results showed that CO-0 samples decreased 3T3 viability at all concentrations and were toxic especially at 100, 75, 50 and 10 µg/mL, cells deteriorated and detached upon incubation with CO-0 samples. Similarly,

in our previous study, plain gelatin samples caused detachment of L929 cells [62]. Therefore, scratch assay could not be carried out any further with CO-0 samples.

On the other hand, cells survived and migration of cells towards the scratch was observed when 3T3 cells were incubated with samples containing CO within 5-100 µg/mL concentration range (Figure 9c, d, e) as CO was previously shown to increase *in vivo* wound healing due to fibroblast proliferation and neovascularization [57]. In our preliminary study, constant CO in gelatin was also shown to also cause healing of L929 cells [62]. In this study, the highest closure of the scratch was observed on 3T3 cell lines incubated with 25 µg/mL concentration of CO incorporated samples especially CO-3 and CO-4 after 24 h of incubation similar to FBS containing positive control group (Figure 9b). This result is in accordance with the XTT results since cell viability was significantly > 100% for all CO incorporated samples at 25 µg/mL concentration ($p < 0.05$).

4. Conclusion

In this study, different amounts of CO were incorporated into gelatin-based films by solution casting method to prepare wound dressing materials with natural components. The influence of CO on various protein-based film properties were compared to determine the sole effect of increasing CO. The results showed that various amounts of CO formed homogenous and continuous plasticized gelatin films without a significant loss of transparency (Figure 1). Heterogeneous and rough surfaces of CO incorporated films were demonstrated by SEM Analysis (Figure 3) which also mainly decreased mechanical strength of the films (Table 3) similar to other studies in the literature [31, 60]. Increasing CO amount decreased TS and YM since oil incorporation at certain amounts is claimed to reduce polymer interactions decreasing rigidity [79,80]. Although CO caused rough surfaces specifically in CO-3 films, no pores were present in CO-4 due to the bigger clustered oil droplets which is also shown by optical microscopy films (Figure 2). Therefore, it can be concluded that increased CO ratio in films may have filled the film surface preventing pore formation due to its plasticizing effect since EAB of CO-4 was more than CO-3 (Table 3). Despite the hydrophobicity of oil, water and saline solution uptake of CO-2, CO-3 and CO-4 films were > 100% after 3 h in both media. CO also improved gelatin films' durability in water and saline solution since aging of CO-4 films was > 10% lower than CO-0 films in both media. FTIR showed that the amplitude of the significant band identified from triglycerides increased as the amount of CO increased in the films. Moreover, protein-protein interaction increased with a decreasing number of free-amino groups as amide-A band shifted to a lower frequency with decreasing amplitudes in CO containing films. Amide-I band of CO-2 was at a lower frequency showing more hydrogen bonding of C=O which may also have caused a higher T_{max} (Figure 6) and stronger mechanical properties of CO-2 among CO incorporated films. DSC showed that incorporation of CO increased T_g of films and influenced crystallization of the films yielding more thermally stable films. XTT showed that increased CO influenced viability of 3T3 cells since CO-2 and CO-3 samples within 5-75 µg/mL; and CO-4 samples at every concentration within 5-100 µg/mL range increased viability, whereas

CO-0 significantly decreased viability at 10, 50, 75, 100 µg/mL ($p < 0.05$; Figure 8). As an indication of wound healing, scratch closure was observed when 3T3 cells were incubated with liquid CO containing biomaterial samples especially at 25 µg/mL concentration shown by *in vitro* Scratch Assay (Figure 9). This study showed that increasing CO amounts mainly improved thermal and healing properties of gelatin-based biomaterial. While CO-2 films had more ideal thermal properties; CO-4 films had better influence on viability and wound healing of 3T3 cell line. Therefore, gelatin-based films containing various amounts of CO, specifically 4:2 and 4:4 (w:w) G:CO, can be suitable candidates for a wound dressing material and can further be explored for *in vivo* tests and for improved mechanical strength in future studies.

Acknowledgements

Authors thank Assoc. Prof. R. Cakir-Koc for giving access to utilize the cell laboratory of Yildiz Technical University.

Disclosure statement

No potential conflict of interest was reported by the authors.

Funding

This study has been funded by Office of Istanbul Gelişim University Scientific Research Projects. (Project number: DUP-220220-MK).

ORCID

Mehlika Karamanlioglu http://orcid.org/0000-0002-4814-6346

References

[1] Che Zain MS, Lee SY, Sarian MN, et al. In vitro wound healing potential of flavonoid c-glycosides from oil palm (*Elaeis guineensis* Jacq.) leaves on 3T3 fibroblast cells. Antioxidants. 2020;9(4):326. doi: 10.3390/antiox9040326.

[2] Sezer AD, Cevher E. Biopolymers as wound healing materials: challenges and new strategies. In: Pignatello R, editor. Biomater appl nanomedicine. Rijeka: Intechopen; 2011. p. 383–414. doi: 10.5772/25177.

[3] Jenkins HP, Clarke JS. Gelatin sponge, a new hemostatic substance: studies on absorbability. Arch Surg (1920). 1945;51(4):253–261. doi: 10.1001/archsurg.1945.01230040262005.

[4] Wang C, Zhu F, Cui Y, et al. An easy-to-use wound dressing gelatin-bioactive nanoparticle gel and its preliminary in vivo study. J Mater Sci Mater Med. 2017;28(1):10. doi: 10.1007/s10856-016-5823-1.

[5] Mogoşanu GD, Grumezescu AM. Natural and synthetic polymers for wounds and burns dressing. Int J Pharm. 2014;463(2):127–136. doi: 10.1016/j.ijpharm.2013.12.015.

[6] Miguez-Pacheco V, Hench LL, Boccaccini AR. Bioactive glasses beyond bone and teeth: emerging applications in contact with soft tissues. Acta Biomater. 2015;13:1–15. doi: 10.1016/j.actbio.2014.11.004.

[7] Demirci GT, Mansur AT, Özker E, et al. Burn treatment with transparent polyurethane wound dressing (omiderm): two case reports. Turkiye Klinikleri J Dermatol. 2017;27(1):51–55. http://www.turkiyeklinikleri.com/article/en-burn-treatment-with-transparent-polyurethane-wound-dressing-omiderm-two-case-reports-74057.html. doi: 10.5336/dermato.2016-49979.

[8] Qu J, Zhao X, Liang Y, et al. Antibacterial adhesive injectable hydrogels with rapid self-healing, extensibility and compressibility as wound dressing for joints skin wound healing. Biomaterials. 2018;183:185–199. doi: 10.1016/j.biomaterials.2018.08.044.

[9] Vowden K, Vowden P. Wound dressings: principles and practice. Surg (United Kingdom). 2017;35(9):489–494. doi: 10.1016/j.mpsur.2017.06.005.

[10] Alven S, Aderibigbe BA. Chitosan and cellulose-based hydrogels for wound management. Int J Mol Sci. 2020;21:1–30.

[11] Sahana TG, Rekha PD. Biopolymers: applications in wound healing and skin tissue engineering. Mol Biol Rep. 2018;45(6):2857–2867. doi: 10.1007/s11033-018-4296-3.

[12] Brett D. A review of collagen and collagen-based wound dressings. Wounds. 2008;20:347–356.

[13] Huang Y, Zhao X, Zhang Z, et al. Degradable gelatin-based IPN cryogel hemostat for rapidly stopping deep noncompressible hemorrhage and simultaneously improving wound healing. Chem. Mater. 2020;32(15):6595–6610. doi: 10.1021/acs.chemmater.0c02030.

[14] Parvez S, Rahman MM, Khan MA, et al. Preparation and characterization of artificial skin using chitosan and gelatin composites for potential biomedical application. Polym. Bull. 2012;69(6):715–731. doi: 10.1007/s00289-012-0761-7.

[15] Zaman HU, Islam JMM, Khan MA, et al. Physico-mechanical properties of wound dressing material and its biomedical application. J Mech Behav Biomed Mater. 2011;4(7):1369–1375. doi: 10.1016/j.jmbbm.2011.05.007.

[16] Ndlovu SP, Ngece K, Alven S, et al. Gelatin-based hybrid scaffolds: promising wound dressings. Polymers (Basel). 2021;13(17):2959. doi: 10.3390/polym13172959.

[17] Akhavan-Kharazian N, Izadi-Vasafi H. Preparation and characterization of chitosan/gelatin/nanocrystalline cellulose/calcium peroxide films for potential wound dressing applications. Int J Biol Macromol. 2019;133:881–891. doi: 10.1016/j.ijbiomac.2019.04.159.

[18] Taheri P, Jahanmardi R, Koosha M, et al. Physical, mechanical and wound healing properties of chitosan/gelatin blend films containing tannic acid and/or bacterial nanocellulose. Int J Biol Macromol. 2020;154:421–432. doi: 10.1016/j.ijbiomac.2020.03.114.

[19] Venien A, Levieux D. Differentiation of bovine from porcine gelatines using polyclonal anti-peptide antibodies in indirect and competitive indirect ELISA. J Pharm Biomed Anal. 2005;39(3-4):418–424. doi: 10.1016/j.jpba.2005.04.013.

[20] Shahram E, Sadraie SH, Kaka G, et al. Evaluation of chitosan–gelatin films for use as postoperative adhesion barrier in rat cecum model. Int J Surg. 2013;11(10):1097–1102. doi: 10.1016/j.ijsu.2013.09.012.

[21] Kavoosi G, Rahmatollahi A, Mohammad Mahdi Dadfar S, et al. Effects of essential oil on the water binding capacity, physico-mechanical properties, antioxidant and antibacterial activity of gelatin films. Lwt-Food Sci Technol [Internet]. 2014;57(2):556–561. doi: 10.1016/j.lwt.2014.02.008.

[22] Amadori S, Torricelli P, Rubini K, et al. Effect of sterilization and crosslinking on gelatin films. J Mater Sci Mater Med. 2015;26:1–9.

[23] Fernández-Pan I, Royo M, Ignacio MJ. Antimicrobial activity of whey protein isolate edible films with essential oils against food spoilers and foodborne pathogens. J Food Sci. 2012;77(7):M383–M390. doi: 10.1111/j.1750-3841.2012.02752.x.

[24] Bahram S, Rezaei M, Soltani M, et al. Whey protein concentrate edible film activated with cinnamon essential oil. J Food Process Preserv. 2014;38(3):1251–1258. doi: 10.1111/jfpp.12086.

[25] Campo C D, Pagno CH, Costa TMH, et al. Gelatin capsule waste: new source of protein to develop a biodegradable film. Polímeros. 2017;27(2):100–107. doi: 10.1590/0104-1428.2371.
[26] Kilinc D, Ocak B, Özdestan-Ocak Ö. Preparation, characterization and antioxidant properties of gelatin films incorporated with *Origanum onites* L. essential oil. Food Measure. 2021;15(1):795–806. doi: 10.1007/s11694-020-00683-y.
[27] Yeddes W, Djebali K, Wannes WA, et al. Gelatin-chitosan-pectin films incorporated with rosemary essential oil: optimized formulation using mixture design and response surface methodology. Int J Biol Macromol. 2020;154:92–103. doi: 10.1016/j.ijbiomac.2020.03.092.
[28] Tongnuanchan P, Benjakul S, Prodpran T. Structural, morphological and thermal behaviour characterisations of fish gelatin film incorporated with basil and citronella essential oils as affected by surfactants. Food Hydrocoll [Internet]. 2014;41:33–43. doi: 10.1016/j.foodhyd.2014.03.015.
[29] Sultan M, Elsayed H, Abdelhakim AEF, et al. Active packaging gelatin films based on chitosan/arabic gum/coconut oil pickering nano emulsions. J Appl Polym Sci. 2022;139:1–18.
[30] Binsi PK, Ravishankar CN, Srinivasa Gopal TK. Development and characterization of an edible composite film based on chitosan and virgin coconut oil with improved moisture sorption properties. J Food Sci. 2013;78(4):E526–E534. doi: 10.1111/1750-3841.12084.
[31] Ismail NA, Mohamad SF, Ibrahim MA, et al. Evaluation of gellan gum film containing virgin coconut oil for transparent dressing materials. Adv Biomater. 2014;2014:1–12. doi: 10.1155/2014/351248.
[32] Marina AM, Che Man YB, Nazimah SAH, et al. Chemical properties of virgin coconut oil. J Am Oil Chem Soc. 2009;86(4):301–307. doi: 10.1007/s11746-009-1351-1.
[33] Ghani NAA, Channip A, Chok Hwee Hwa P, et al. Physicochemical properties, antioxidant capacities, and metal contents of virgin coconut oil produced by wet and dry processes. Food Sci Nutr. 2018;6(5):1298–1306. doi: 10.1002/fsn3.671.
[34] Verallo-Rowell VM, Dillague KM, Syah-Tjundawan BS. Novel antibacterial and emollient effects of coconut and virgin olive oils in adult atopic dermatitis. Dermatitis. 2008;19(6):308–315. doi: 10.2310/6620.2008.08052.
[35] Sachs M, Von Eichel J, Asskali F. Wound management with coconut oil in Indonesian folk medicine. Chirurg. 2002;73(4):387–392. doi: 10.1007/s00104-001-0382-4.
[36] Intahphuak S, Khonsung P, Panthong A. Anti-inflammatory, analgesic, and antipyretic activities of virgin coconut oil. Pharm Biol. 2010;48(2):151–157. doi: 10.3109/13880200903062614.
[37] Vaughn AR, Clark AK, Sivamani RK, et al. Natural oils for skin-barrier repair: ancient compounds now backed by modern science. Am J Clin Dermatol. 2018;19(1):103–117. doi: 10.1007/s40257-017-0301-1.
[38] Peedikayil FC, Remy V, John S, et al. Comparison of antibacterial efficacy of coconut oil and chlorhexidine on *Streptococcus mutans*: an in vivo study. J Int Soc Prev Community Dent. 2016;6(5):447–452. doi: 10.4103/2231-0762.192934.
[39] DebMandal M, Mandal S. Coconut (*Cocos nucifera* L.: Arecaceae): in health promotion and disease prevention. Asian Pac J Trop Med. 2011;4(3):241–247. doi: 10.1016/S1995-7645(11)60078-3.
[40] Dayrit FM. The properties of lauric acid and their significance in coconut oil. J Americ Oil Chem Soc. 2015;92(1):1–15. doi: 10.1007/s11746-014-2562-7.
[41] Hierholzer JC, Kabara JJ. In vitro effects of monolaurın compounds on enveloped RNA and DNA viruses. J Food Saf. 1982;4(1):1–12. doi: 10.1111/j.1745-4565.1982.tb00429.x.
[42] Shino B, Peedikayil FC, Jaiprakash SR, et al. Comparison of antimicrobial activity of chlorhexidine, coconut oil, probiotics, and ketoconazole on *Candida albicans* isolated in children with early childhood caries: an in vitro study. Scientifica (Cairo). 2016;2016:7061587. doi: 10.1155/2016/7061587.
[43] Kamdem SS, Guerzoni ME, Baranyi J, et al. Effect of capric, lauric and α-linolenic acids on the division time distributions of single cells of *Staphylococcus aureus*. Int J Food Microbiol. 2008;128(1):122–128. doi: 10.1016/j.ijfoodmicro.2008.08.002.

[44] Shilling M, Matt L, Rubin E, et al. Antimicrobial effects of virgin coconut oil and its medium-chain fatty acids on clostridium difficile. J Med Food. 2013;16(12):1079–1085. doi: 10.1089/jmf.2012.0303.
[45] Wang J, Wang X, Li J, et al. Effects of dietary coconut oil as a medium-chain fatty acid source on performance, carcass composition and serum lipids in male broilers. Asian-Australas J Anim Sci. 2015;28(2):223–230. doi: 10.5713/ajas.14.0328.
[46] Srivastava Y, Semwal AD, Sajeevkumar VA, et al. Melting, crystallization and storage stability of virgin coconut oil and its blends by differential scanning calorimetry (DSC) and Fourier transform infrared spectroscopy (FTIR). J Food Sci Technol. 2017;54(1):45–54. doi: 10.1007/s13197-016-2427-1.
[47] Deen A, Visvanathan R, Wickramarachchi D, et al. Chemical composition and health benefits of coconut oil: an overview. J Sci Food Agric. 2021;101(6):2182–2193. doi: 10.1002/jsfa.10870.
[48] Witcher KJ, Novick RP, Schlievert PM. Modulation of immune cell proliferation by glycerol monolaurate. Clin Diagn Lab Immunol. 1996;3(1):10–13. doi: 10.1128/cdli.3.1.10-13.1996.
[49] Pereira CCB, Da Silva MAP, Langone MAP. Enzymatic synthesis of monolaurin. Proc Twenty-Fifth symp biotechnol fuels chem held May 4–7., 2003, Breckenridge, CO. Springer; 2004. p. 433–445.
[50] Bergsson G, Steingrímsson O, Thormar H. Bactericidal effects of fatty acids and monoglycerides on *Helicobacter pylori*. Int J Antimicrob Agents. 2002;20(4):258–262. doi: 10.1016/s0924-8579(02)00205-4.
[51] Srivastava Y, Semwal AD, Sharma GK. Virgin coconut oil as functional oil. In: Grumezescu AM, Holban AM, editors. Ther probiotic, unconv foods. London, UK: Academic Press; 2018. p. 291–301. doi: 10.1016/B978-0-12-814625-5.00015-7.
[52] Thormar H, Isaacs CE, Brown HR, et al. Inactivation of enveloped viruses and killing of cells by fatty acids and monoglycerides. Antimicrob Agents Chemother. 1987;31(1):27–31. doi: 10.1128/AAC.31.1.27.
[53] Yuhas R, Pramuk K, Lien EL. Human milk fatty acid composition from nine countries varies most in DHA. Lipids. 2006;41(9):851–858. doi: 10.1007/s11745-006-5040-7.
[54] Newburg DS, Walker WA. Protection of the neonate by the innate immune system of developing gut and of human milk. Pediatr Res. 2007;61(1):2–8. doi: 10.1203/01.pdr.0000250274.68571.18.
[55] Carpo BG, Verallo-Rowell VM, Kabara J. Novel antibacterial activity of monolaurin compared with conventional antibiotics against organisms from skin infections: an in vitro study. J Drugs Dermatology JDD. 2007;6:991–998.
[56] Mohamadi PS, Hivechi A, Bahrami H, et al. Antibacterial and biological properties of coconut oil loaded poly(ε-caprolactone)/gelatin electrospun membranes. J Ind Text. 2022;51(1_suppl):906S–930S. doi: 10.1177/1528083721991595.
[57] Nevin KG, Rajamohan T. Effect of topical application of virgin coconut oil on skin components and antioxidant status during dermal wound healing in young rats. Skin Pharmacol Physiol. 2010;23(6):290–297. doi: 10.1159/000313516.
[58] Mohamadi PS, Hivechi A, Bahrami SH, et al. Fabrication and investigating in vivo wound healing property of coconut oil loaded nanofiber/hydrogel hybrid scaffold. Biomater Adv. 2022;142:213139. doi: 10.1016/j.bioadv.2022.213139.
[59] Muktar MZ, Rose LBC, Amin KAM. Formulation and optimization of virgin coconut oil with tween-80 incorporated in gellan gum hydrogel. AIP Conf Proc. 2017;1885:020044.
[60] Ismail NA, Amin KAM, Razali MH. Mechanical and antibacterial activities study of gellan gum/virgin coconut oil film embedded norfloxacin. IOP Conf Ser Mater Sci Eng. 2018;440:12001.
[61] Muktar MZ, Ismail WIW, Razak SIA, et al. Accelerated wound healing of physically cross linked gellan gum-virgin coconut oil hydrogel containing manuka honey. ASM Sci J. 2018;11:166–182.

[62] Karamanlioglu M, Yesilkir-Baydar S. Production and characterization of a coconut oil incorporated gelatin-based film and its potential biomedical application. Biomed. Mater. 2022;17(4):045014. doi: 10.1088/1748-605X/ac6c67.
[63] Hong H, Liu C, Wu W. Preparation and characterization of chitosan/PEG/gelatin composites for tissue engineering. J. Appl. Polym. Sci. 2009;114(2):1220–1225. doi: 10.1002/app.30619.
[64] Jarockyte G, Daugelaite E, Stasys M, et al. Accumulation and toxicity of superparamagnetic iron oxide nanoparticles in cells and experimental animals. IJMS. 2016;17(8):1193. doi: 10.3390/ijms17081193.
[65] Meliala DIP, Silalahi J, Yuandani Y, et al. The role of coconut oil to increase expression of MMP-9, PDGF-BB, and TGF-β1 in NIH-3t3 cell line. Open Access Maced J Med Sci. 2019;7(22):3733–3736. doi: 10.3889/oamjms.2019.492.
[66] Chen Y. Scratch wound healing assay. Bio-protocol. 2012;2(5):e100. doi: 10.21769/BioProtoc.100.
[67] Vanin FM, Sobral PJA, Menegalli FC, et al. Effects of plasticizers and their concentrations on thermal and functional properties of gelatin-based films. Food Hydrocoll. 2005;19(5):899–907. doi: 10.1016/j.foodhyd.2004.12.003.
[68] Varma RK, Kaushal R, Junnarkar AY, et al. Polysorbate 80: a pharmacological study. Arzneimittelforschung. 1985;35(5):804–808.
[69] Samadi A, Azandeh S, Orazizadeh M, et al. Fabrication and characterisation of chitosan/polyvinyl alcohol-based transparent hydrogel films loaded with silver nanoparticles and sildenafil citrate for wound dressing applications. Mater Technol. 2022;37:355–365. doi: 10.1080/10667857.2020.1842151.
[70] Liakos I, Rizzello L, Hajiali H, et al. Fibrous wound dressings encapsulating essential oils as natural antimicrobial agents. J Mater Chem B. 2015;3(8):1583–1589. doi: 10.1039/c4tb01974a.
[71] Rosa JM, Bonato LB, Mancuso CB, et al. Antimicrobial wound dressing films containing essential oils and oleoresins of pepper encapsulated in sodium alginate films. Cienc. Rural. 2018;48(3):1–5. doi: 10.1590/0103-8478cr20170740.
[72] Wang YW, Wu Q, Chen GQ. Reduced mouse fibroblast cell growth by increased hydrophilicity of microbial polyhydroxyalkanoates via hyaluronan coating. Biomaterials. 2003;24(25):4621–4629. doi: 10.1016/s0142-9612(03)00356-9.
[73] Ma W, Tang CH, Yin SW, et al. Effect of homogenization conditions on properties of gelatin-olive oil composite films. J Food Eng [Internet]. 2012;113(1):136–142. doi: 10.1016/j.jfoodeng.2012.05.007.
[74] Atarés L, Bonilla J, Chiralt A. Characterization of sodium caseinate-based edible films incorporated with cinnamon or ginger essential oils. J Food Eng. 2010;100(4):678–687. doi: 10.1016/j.jfoodeng.2010.05.018.
[75] Mao J, Zhao L, De Yao K, et al. Study of novel chitosan-gelatin artificial skin in vitro. J Biomed Mater Res Part A an off J Soc Biomater Japanese Soc Biomater Aust Soc Biomater Korean Soc Biomater. 2003;64:301–308.
[76] Rosli NA, Ahmad I, Anuar FH, et al. The contribution of eco-friendly bio-based blends on enhancing the thermal stability and biodegradability of poly (lactic acid). J Clean Prod. 2018;198:987–995. doi: 10.1016/j.jclepro.2018.07.119.
[77] Lee KY, Shim J, Lee HG. Mechanical properties of gellan and gelatin composite films. Carbohydr Polym. 2004;56(2):251–254. doi: 10.1016/j.carbpol.2003.04.001.
[78] Zinoviadou KG, Koutsoumanis KP, Biliaderis CG. Physico-chemical properties of whey protein isolate films containing oregano oil and their antimicrobial action against spoilage flora of fresh beef. Meat Sci. 2009;82(3):338–345. doi: 10.1016/j.meatsci.2009.02.004.
[79] Tongnuanchan P, Benjakul S, Prodpran T. Properties and antioxidant activity of fish skin gelatin film incorporated with citrus essential oils. Food Chem. 2012;134(3):1571–1579. doi: 10.1016/j.foodchem.2012.03.094.

[80] Limpisophon K, Tanaka M, Osako K. Characterisation of gelatin-fatty acid emulsion films based on blue shark (*Prionace glauca*) skin gelatin. Food Chem [Internet]. 2010;122(4):1095–1101. doi: 10.1016/j.foodchem.2010.03.090.
[81] Muyonga JH, Cole CGB, Duodu KG. Characterisation of acid soluble collagen from skins of young and adult nile perch (*Lates niloticus*). Food Chem. 2004;85(1):81–89. doi: 10.1016/j.foodchem.2003.06.006.
[82] Hoque MS, Benjakul S, Prodpran T. Effect of heat treatment of film-forming solution on the properties of film from cuttlefish (*Sepia pharaonis*) skin gelatin. J Food Eng. 2010;96(1):66–73. doi: 10.1016/j.jfoodeng.2009.06.046.
[83] Chuaynukul K, Nagarajan M, Prodpran T, et al. Comparative characterization of bovine and fish gelatin films fabricated by compression molding and solution casting methods. J Polym Environ. 2018;26(3):1239–1252. doi: 10.1007/s10924-017-1030-5.
[84] Xie Y, Zhou H, Qian H. Effect of addition of peach gum on physicochemical properties of gelatin-based microcapsule. J Food Biochemistry. 2006;30(3):302–312. doi: 10.1111/j.1745-4514.2006.00061.x.
[85] Das MP, R SP, Prasad K, et al. Extraction and characterization of gelatin: a functional biopolymer. Int J Pharm Pharm Sci. 2017;9(9):239. doi: 10.22159/ijpps.2017v9i9.17618.
[86] Bergo P, Sobral PJA. Effects of plasticizer on physical properties of pigskin gelatin films. Food Hydrocoll. 2007;21(8):1285–1289. doi: 10.1016/j.foodhyd.2006.09.014.
[87] Ma W, Tang CH, Yin SW, et al. Characterization of gelatin-based edible films incorporated with olive oil. Food Res Int. 2012;49(1):572–579. doi: 10.1016/j.foodres.2012.07.037.
[88] Guillen MD, Cabo N. Characterization of edible oils and lard by fourier transform infrared spectroscopy. Relationships between composition and frequency of concrete bands in the fingerprint region. J Americ Oil Chem Soc. 1997;74(10):1281–1286. doi: 10.1007/s11746-997-0058-4.
[89] Guillén MD, Cabo N. Relationships between the composition of edible oils and lard and the ratio of the absorbance of specific bands of their Fourier transform infrared spectra. Role of some bands of the fingerprint region. J. Agric. Food Chem. 1998;46(5):1788–1793. doi: 10.1021/jf9705274.
[90] Guillén MD, Cabo N. Study of the effects of smoke flavourings on the oxidative stability of the lipids of pork adipose tissue by means of Fourier transform infrared spectroscopy. Meat Sci. 2004;66(3):647–657. doi: 10.1016/S0309-1740(03)00185-2.
[91] Wong DP, Chua MT, Enriquez EP. Composition ot glvceride esters of lauric acid bV FTIR band shape analysis. KIMIKA. 2006;22:7–14.
[92] Rohman A, Che Man YB, Ismail A, et al. Application of FTIR spectroscopy for the determination of virgin coconut oil in binary mixtures with olive oil and palm oil. J Americ Oil Chem Soc. 2010;87(6):601–606. doi: 10.1007/s11746-009-1536-7.
[93] Sobral PJA, Menegalli F, Hubinger MD, et al. Mechanical, water vapor barrier and thermal properties of gelatin based edible films. Food Hydrocoll. 2001;15(4-6):423–432. doi: 10.1016/S0268-005X(01)00061-3.
[94] Slade L, Levine H. Polymer-chemical properties of gelatin in foods. In: Pearson AM, Dutson TR, Bailey AJ, editors. Adv Meat Res. Vol.4. New York: AVI; 1987; p. 251–266.
[95] Wellen RMR, Canedo EL, Rabello MS. Melting and crystallization of poly(3-hydroxybutyrate)/carbon black compounds. Effect of heating and cooling cycles on phase transition. J. Mater. Res. 2015;30(21):3211–3226. doi: 10.1557/jmr.2015.287.
[96] Słota D, Florkiewicz W, Piętak K, et al. Preparation, characterization, and biocompatibility assessment of polymer-ceramic composites loaded with salvia officinalis extract. Materials. 2021;14:6000. doi: 10.3390/ma14206000.
[97] Yousefi K, Hamedeyazdan S, Hodaei D, et al. An in vitro ethnopharmacological study on prangos ferulacea: a wound healing agent. Bioimpacts. 2017;7(2):75–82. doi: 10.15171/bi.2017.10.
[98] Çınar İ. Gossypin'in L929 fibroblast hücrelerindeki hidrojen peroksit hasarına karşı koruyucu etkilerinin değerlendirilmesi. Kafkas J Med Sci. 2020;10(1):15–23. doi: 10.5505/kjms.2020.06025.

[99] Walter MNM, Wright KT, Fuller HR, et al. Mesenchymal stem cell-conditioned medium accelerates skin wound healing: an in vitro study of fibroblast and keratinocyte scratch assays. Exp Cell Res. 2010;316(7):1271–1281. doi: 10.1016/j.yexcr.2010.02.026.
[100] Baktir G. Wound repair and experimental wound models. Experimed. 2020;9(3):130–137. doi: 10.26650/experimed.2019.19023.
[101] Fronza M, Heinzmann B, Hamburger M, et al. Determination of the wound healing effect of calendula extracts using the scratch assay with 3T3 fibroblasts. J Ethnopharmacol. 2009;126(3):463–467. https://www.sciencedirect.com/science/article/pii/S0378874109005741. doi: 10.1016/j.jep.2009.09.014.
[102] Yin M, Wan S, Ren X, et al. Development of inherently antibacterial, biodegradable, and biologically active chitosan/pseudo-protein hybrid hydrogels as biofunctional wound dressings. ACS Appl Mater Interfaces. 2021;13(12):14688–14699. doi: 10.1021/acsami.0c21680.
[103] Agarwal A, Weis TL, Schurr MJ, et al. Surfaces modified with nanometer-thick silver-impregnated polymeric films that kill bacteria but support growth of mammalian cells. Biomaterials. 2010;31(4):680–690. doi: 10.1016/j.biomaterials.2009.09.092.
[104] Gratzner HG. Monoclonal antibody to 5-bromo-and 5-iododeoxyuridine: a new reagent for detection of DNA replication. Science. 1982;218(4571):474–475. doi: 10.1126/science.7123245.
[105] Khan Y. Characterizing the properties of tissue constructs for regenerative engineering. In: Narayan RBT-E of BE, editor. Encycl biomed eng. Oxford: Elsevier; 2019. p. 537–545. https://www.sciencedirect.com/science/article/pii/B9780128012383998970.
[106] Seleem D, Chen E, Benso B, et al. In vitro evaluation of antifungal activity of monolaurin against *Candida albicans* biofilms. PeerJ. 2016;4:e2148. doi: 10.7717/peerj.2148.
[107] Rodriguez LG, Wu X, Guan J-L. Wound-healing assay. In: Guan J-L, editor. Methods Mol. Biol. Vol. 294. Totowa, New Jersey: Humana Press; 2005. p. 23–29. doi: 10.1385/1-59259-860-9:023.
[108] Cory G. Scratch-wound assay. In: Wells CM, Parsons M, editors. Methods Mol Biol. Vol. 769. Totowa, New Jersey: Humana Press; 2011. p. 25–30. doi: 10.1007/978-1-61779-207-6_2.
[109] Smith MJ, Dempsey SG, Veale RWF, et al. Further structural characterization of ovine forestomach matrix and multi-layered extracellular matrix composites for soft tissue repair. J Biomater Appl. 2022;36(6):996–1010. doi: 10.1177/08853282211045770.
[110] Qadir A, Jahan S, Aqil M, et al. Phytochemical-based nano-pharmacotherapeutics for management of burn wound healing. Gels. 2021;7(4):209. doi: 10.3390/gels7040209.
[111] Malinda KM, Sidhu GS, Banaudha KK, et al. Thymosin α1 stimulates endothelial cell migration, angiogenesis, and wound healing. J Immunol. 1998;160(2):1001–1006. doi: 10.4049/jimmunol.160.2.1001.
[112] Öztopalan DF, Işık R, Durmuş AS. Yara iyileşmesinde büyüme faktörleri ve sitokinlerin rolü. Dicle Üniversitesi Vet Fakültesi Derg. 2017;10:83–88.
[113] Feoktistova M, Geserick P, Leverkus M. Crystal violet assay for determining viability of cultured cells. Cold Spring Harb Protoc. 2016;2016(4):pdb.prot087379. doi: 10.1101/pdb.prot087379.